

Benchmarking UWB-Based Infrastructure-Free Positioning and Multi-Robot Relative Localization: Dataset and Characterization

Paola Torrico Morón[†], Sahar Salimpour[†], Lei Fu[†], Xianjia Yu[†], Jorge Peña Queralta[†], Tomi Westerlund[†]

[†]Turku Intelligent Embedded and Robotic Systems (TIERS) Lab, University of Turku, Finland.

Emails: ¹{pctomo, sahar, leifu, xianjia.yu, jopequ, toveve}@utu.fi

Abstract—Ultra-wideband (UWB) positioning has emerged as a low-cost and dependable localization solution for multiple use cases, from mobile robots to asset tracking within the Industrial IoT. The technology is mature and the scientific literature contains multiple datasets and methods for localization based on fixed UWB nodes. At the same time, research in UWB-based relative localization and infrastructure-free localization is gaining traction, further domains, tools and datasets in this domain are scarce. Therefore, we introduce in this paper a novel dataset for benchmarking infrastructure-free relative localization targeting the domain of multi-robot systems. Compared to previous datasets, we analyze the performance of different relative localization approaches for a much wider variety of scenarios with varying numbers of fixed and mobile nodes. A motion capture system provides ground truth data, are multi-modal and include inertial or odometry measurements for benchmarking sensor fusion methods. Additionally, the dataset contains measurements of ranging accuracy based on the relative orientation of antennas and a comprehensive set of measurements for ranging between a single pair of nodes. Our experimental analysis shows that high accuracy can be localization, but the variability of the ranging error is significant across different settings and setups.

Index Terms—UAV; GNSS; Ultra-wideband; UWB; VIO; Localization; MAV; UGV; Cooperative localization; Navigation;

I. INTRODUCTION

Over the last years, autonomous robots have become more popular in society. As a result, the need for connectivity and networked collaborative systems has gained increasing importance [1]. Their autonomous operations are usually supported by GNSS sensors such as GPS [2]. There are, however, several scenarios where robots need to operate in GNSS-denied environments. Warehouses [3], construction [4], and mining, for example, require different approaches.

A popular approach to the localization problem in such scenarios is the use of visual sensors such as cameras. This is due to their low cost and flexibility [5]. A common solution includes visual-inertial odometry with either monocular cameras [6] or multiple sensors [7]. Other solutions include onboard sensors such as IMUs[8] or odometry estimation from Lidars [9]. Either of the presented solutions however has its limitations. Visual cameras are affected by the light conditions of the environment, and dust or smoke present affects visibility even more [10]. On the other hand, IMUs are affected by



Fig. 1: Different rotations for an UWB node. Yaw, pitch and roll plane of rotations respectively for UWB error characterization

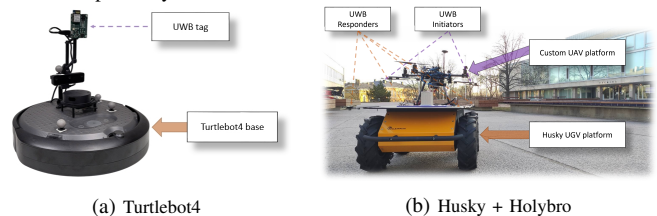


Fig. 2: Robots used for the data collection for the dataset. Figure 2a shows a Turtlebot4 mounted with a UWB module. Figure 2b shows a Husky with a landing platform and a custom UAV equipped with two UWBs.

long-term drifts and LiDARs by the lack of clearly defined structures [11].

As a solution to overcome the challenges with visual-based localization caused by environmental conditions, ultra-wideband (UWB) technology has emerged as a promising alternative for robot localization [12]. In recent years, there has been a significant increase in research on UWB-based relative localization in GNSS-denied environments, which aims to eliminate the requirements for stationary anchors [13]. It has been particularly useful in multi-robot systems to achieve accurate and robust position estimation without the need for external infrastructure. We will be presenting some of the existing datasets for UWB localization as background for the construction of our dataset.

In this work, we will present the different cases of UWB data collection for error characterization and localization. We present the details of data acquisition in each case as well as some analysis of the results, both for the errors as well as the localization solutions implemented. The dataset will present different scenarios, focusing on infrastructure-free positioning and multi-robot relative localization, with the data acquired capable of being implemented in multi-robot solutions. We

also present different spatial configurations.

The rest of the document is organized as follows. Section II reviews the background of UWB localization and presents existing datasets with UWB localization. Section III presents different relative localization methods. Section IV presents the methodology used for data acquisition and the subsets present in the dataset. Section V presents an analysis of the dataset, with error characterization, positioning error, and localization algorithm comparison. Finally, section VI presents the conclusions.

II. BACKGROUND

Through this section, we discuss the existing works on UWB localization datasets and methods. A detailed comparison of our dataset with others is shown in Table I.

Bregar et al. introduced in [14] a method to reduce the localization error for non-line-of-sight (NLOS) conditions by utilizing convolutional neural networks (CNNs) or ranging error regression models and analyzing the Channel Impulse Response (CIR) of the UWB in unknown environments. They utilize DWM1000 modules using four as anchors and one as a tag while implementing Time of Flight (ToF) ranging. Bregar et al. build a dataset of measurements from the tag to each anchor and the known distances for training the CNN.

Li et al. employed in [15] an Extended Kalman Filter (EKF) to fuse UWB and IMU data. Based on known distances and angles, the author implements six fixed UWB anchors using PulsON P440. Using Time of Arrival (TOA) a micro aerial vehicle (MAV) equipped with a UWB was able to autonomously track a path in the environment.

Barral et al. in [16] present the dataset to study the feasibility of utilizing UWB technology in an industrial setting for tracking forklift trucks. The authors implement DWM1000 UWB devices to record ranging measurements for their UWB gazebo simulator. Measures were taken at different distances in three different scenarios with line-of-sight (LOS) and NLOS. Their simulator then uses fixed anchors and one mobile tag implementing a Kalman Filter approach for localization.

Raza et al. presents in [17] a dataset for intelligent calibration of different localization technologies such as UWB, Bluetooth, and MOCAP from initial calibration. The group uses four anchors and one mobile tag with the DWM1001 modules while using Time Difference of Arrival (TDoA) for the ranging measurements.

Peña [10] et al. present a UWB dataset with twelve subsets of data. They implement three, four, or six anchors for robust localization. Four of the scenarios provided have the UWB anchors in the corner of their testing arena, while the others present different height, number, or placement configurations. They have a moving tag mounted in a quadrotor, moved manually around the testing area, and implement ToF ranging. They utilize DWM1001 UWB modules for all their data acquisition, for studying the localization accuracy with self-calibrating anchor positions.

Delamare [18] et al. provide a dataset for the flow of movement in an industrial site with UWB, however, it is

done with human workers instead of robots. They provide the movements of an entire assembly line with the use of four anchors with known locations and six moving nodes, one per person. Implementing DWM1001 UWB nodes, and tracking movements with the Two Way Ranging (TWR) algorithm provided by Qorvo. Their UWB localization is validated by obtaining ground truth positions using a MOCAP system.

Vey [19] et al. introduce a UWB dataset acquired in a UWB Based Rangin testbed for the Internet of Things. They present a scenario with six anchors also in known locations for LOS and NLOS scenarios. They implement an autonomously moving tag and implement TWR ranging. The UWB ranging and ranging errors are presented in the dataset for the enhancement of localization algorithms and protocols.

III. RELATIVE LOCALIZATION METHODS

In this section, we introduce different methods for relative localization between a series of N UWB nodes without known positions, using multilateration, least squares, and gradient descent techniques.

A. Multilateration

Multilateration is a technique that estimates the position of a node based on the distances or difference of distances between multiple nodes [20]. In the case of UWB-based positioning with N nodes, we can use ToF ranging for distances or TDoA for the difference of distances. Given the distances, the position of an unknown node can be determined by solving a system of equations:

$$\|\mathbf{p}_i - \mathbf{p}_j\| = d_{ij}, \quad i, j = 1, 2, \dots, N \quad (1)$$

where p_i and p_j are the positions of nodes i and j , respectively, and d_{ij} is the distance between them.

B. Least Squares

Least squares is a popular optimization technique that can be used for relative localization [14]. Given a set of distances, we can formulate the localization problem as a least squares optimization problem:

$$\min_{\mathbf{p}_1, \mathbf{p}_2, \dots, \mathbf{p}_n} \sum_{i=1}^n \sum_{j=i+1}^n (\|\mathbf{p}_i - \mathbf{p}_j\| - d_{ij})^2 \quad (2)$$

Solving this optimization problem yields the positions of the nodes that minimize the total squared error between the measured and estimated distances.

C. Gradient Descent

Gradient descent is an iterative optimization algorithm that can be employed for relative localization [21]. In this approach, we start with an initial guess for the node positions and iteratively update the positions based on the gradient of the objective function:

$$\mathbf{p}_i^{(k+1)} = \mathbf{p}_i^{(k)} - \alpha \nabla_{\mathbf{p}_i} J(\mathbf{p}_1, \mathbf{p}_2, \dots, \mathbf{p}_n) \quad (3)$$

TABLE I: Comparison table of existing UWB localization datasets and ours. For each one we include the number of UWB nodes, if they are fixed or mobile, if the data is used for absolute or relative localization, the number of subsets given, if the UWB are inside or outside the convex envelope, the type of UWB utilized and finally if the also present other sensor information.

	#Nodes	#Fixed Nodes	#Mobile Nodes	#Absolute Loc.	#Relative Loc.	Subsets	Convex Envelope	UWB Node	Extra Sensors
Bregar [14](2018)	5	4	1	✓	-	2	In	DWM1000	
Li [15](2018)	7	6	1	✓	-	1	In	PulsON P440	IMU
Barral [16](2019)	8	7	1	✓	-	2	In	Pozyx	
Raza [17](2019)	6	4	3	✓	-	2	In	DWM1001	Bluetooth
Peña [10](2020)	3-6	3-6	1-4	✓	✓	12	In/Out	DWM1001	
Delamare [18](2020)	10	4	6	✓	-	2	In	DWM1001	
Vey [19](2022)	7	6	1	-	-	1	In	DWM1001	
Ours	2-8	2-8	0-5	✓	✓	24	In/Out	DWM1001	VIO

where $p_i^{(k)}$ is the position of node i at iteration k , α is the learning rate, and $J(p_1, p_2, \dots, p_n)$ is the objective function defined in the least squares formulation.

By gradually updating the positions and moving towards the minimum of the error function, gradient descent converges to the final accurate and robust positioning that minimizes the error function.

IV. METHODOLOGY

This section describes the data included in the dataset, and the steps followed for acquiring the data in the different scenarios. All the data and code used for recording it has been made public in Github ¹.

A. Data Acquisition

The dataset presented in this work consists of five different cases. All of them utilize Qorvo’s DWM1001 UWB modules with custom firmware for ToF ranging. Depending on the case, the UWB modules are mounted either in Turtlebot4, a custom platform for the Husky robot or custom UAV shown in Figure 2, or in a known location in the testing arena. All measurements are obtained from the DWM1001 device by UART connection and interfaced with ROS2 nodes for processing and recording. The ground truth for measurements is provided by a MOCAP system of eight Optitrack cameras in a testing arena of $8m \times 9m$ except for Case I, where the area was expanded to $8m \times 16m$.

Each case consists of one or more subsets of data, which are going to be further detailed in the next section. The data acquisition for each case is obtained as follows. *Case I*: is the UWB raw measurements for two UWB devices one set as initiator and one as responder. Measurements were taken for distances between $1m$ to $16m$ with steps of $1m$, and for each of the different rotations in Figure 1. A hundred measurements are taken for each distance and rotation combination. For this case, one UWB is static while the second is moved manually both for the distance and the rotations.

Case II: four UWB modules are fixed in known locations, either in the arena corners or on the platform for the Husky robot. Two UWB modules located in the custom UAV are moved around the arena in different predefined trajectories. The UAV’s modules act as initiators while the other four nodes act as responders. The communication frequency in this case is

38Hz. *Case III*: consists of eight UWB devices mounted in the Turtlebot4 and located in different predefined configurations. They communicate all-to-all, with all taking turns in being initiators and responders. *Case IV*: consists on the datasets utilized for our previous work in [22]. This scenario also utilizes the all-to-all communication with the UWB on the Turtlebots, with two static Turtlebots and five moving ones. Finally, *Case V*: has five Turtlebots equipped with one UWB module and a VIO camera. This case comes from [23] and has one static node and four moving ones. For all the cases implemented in the Turtlebots, the frequency is 15Hz.

B. Data Subsets

Each of the five cases mentioned before consists of one or more subsets of data. *Case I*: has only one subset with the twelve rotations for each of the distances from $1m$ to $16m$. *Case II*: consists of fourteen subsets of data, each with a different responder localization or the initiator trajectory. The initiators in the UAV can be moving either inside the convex envelope created by the four responders or outside it. This will impact the localization implemented for each scenario, with a worse performance when outside the envelope. Some of the scenarios presented in this case can be appreciated in Figure 3.

Case III: has a total of three different configurations for the eight Turtlebot robots, with two being shown in Figure 4. The configurations were chosen because they represent some edge cases for localization and are challenging to solve. In this paper, we present two methods using the solutions from [22]. *Case IV*: consists of four subsets, with the robots moving in the same pattern for each one, and finally *Case V*: has two subsets with the Turtlebots also moving in the same patterns, but this time also with VIO data. A summary table of all the different scenarios for the dataset for each of the cases can be seen in Table II

TABLE II: Description of the Data Subsets for each of the cases presented.

	#UWB Nodes	#Fixed Nodes	#Mobile Nodes	#Resp Nodes	#Init Nodes	#Freq. [Hz]	#Sub.
Case I	2	1	1	1	1	45	1
Case II	6	4	2	4	2	38	14
Case III	8	8	0	8	8	15	3
Case IV	7	2	5	7	7	15	4
Case V	5	1	4	5	5	7	2

¹<https://github.com/TIERS/uwb-relative-localization-dataset>

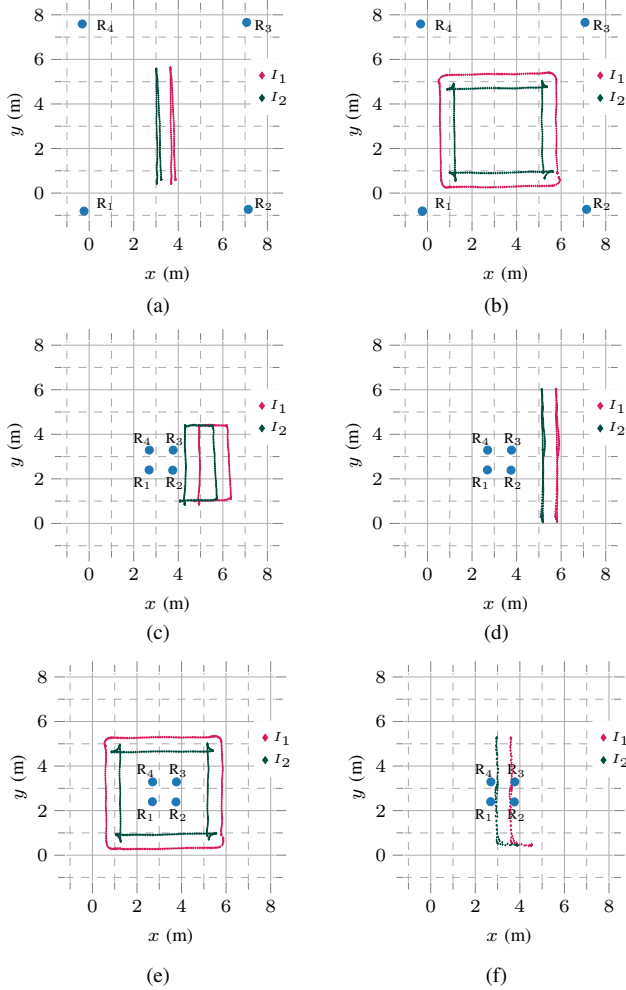


Fig. 3: A subset of the different scenarios for Case II. It presents both the scenarios where the initiators move inside the convex envelope, Figure 3a and Figure 3b, and outside the envelope, Figure 3d, Figure 3c and Figure 3e.

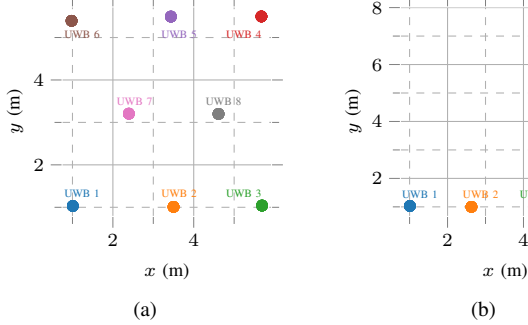


Fig. 4: Different Case III configurations; eight nodes all-to-all communication.

V. DATASET ANALYSIS — UWB CHARACTERIZATION

A. UWB Ranging Error Modeling

In *Case I* we analyzed the distance error obtained by a pair of UWB nodes at different distances and rotations. Figure 5a shows the errors obtained from all the distances when both faces of the UWB are directed at each other. This configuration is considered to be 0° . Overall the error increases as the distance increases, with some outliers at $9m$ and $14m$. On the other hand, Figure 5b shows the relative error in the same

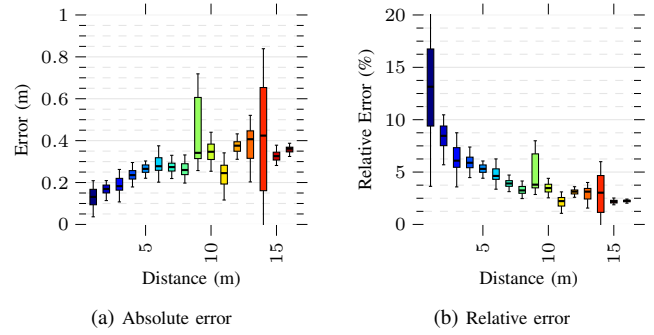


Fig. 5: Absolute and relative distance error for two UWB nodes directly facing each other, rotation 0° , at different distances. Figure 5a shows the absolute error, while Figure 5b shows the relative error.

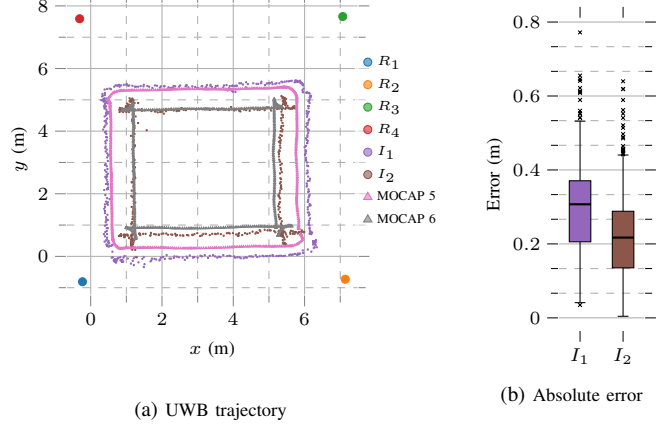


Fig. 6: UWB node localization for two moving UWB Initiators implementing a Least Square Estimator inside the convex envelope alongside the absolute position error.

scenario. In this case, the relative error of the measurements drops when increasing the distance.

We obtained the distance error for the UWB distance for each rotation in Figure 1 at each distance. We only present the absolute error for each scenario which can be seen in Table III. Each row is a different rotation plane and each column has a different angle of rotation, all with the same starting position, angle 0° , that was shown in Figure 5a. Overall, the error in most configurations increases with distance. For Yaw, we can observe the highest errors at 180° . Angles 90° and 270° have similar results, and 0° has the lowest errors. On Pitch, the errors for 90° and 270° have less of a clear upward trend, with 270° having the most fluctuating results overall. The errors for Pitch are also higher than Yaw. For Roll, all angles present an increasing trend. Once again 180° has the highest errors, with 90° and 270° again having similar results.

B. Positioning error

In *Case II* we present different scenarios with four static responders and two mobile initiators. There exist scenarios where the responders are located at the corners of the testing arena, and others where they are in the platform for the Husky and located in the middle. As a result, the two mobile initiators might be moving inside or outside the convex envelope of the responders. We implemented a Least Square Estimator (LSE) to obtain the position of the mobile UWB to the anchors

TABLE III: Absolute distance error of two UWB nodes at different distances when one node is rotated in one of the rotations planes. For clarity, we remove axis labels, with the error in meters in the y axis and the distance between the nodes in meters in the x axis.

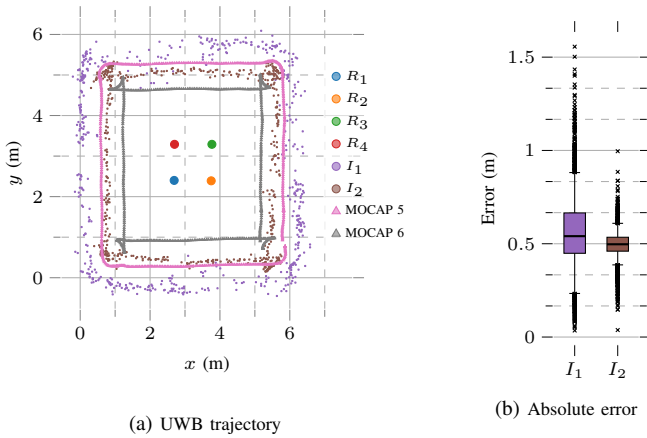
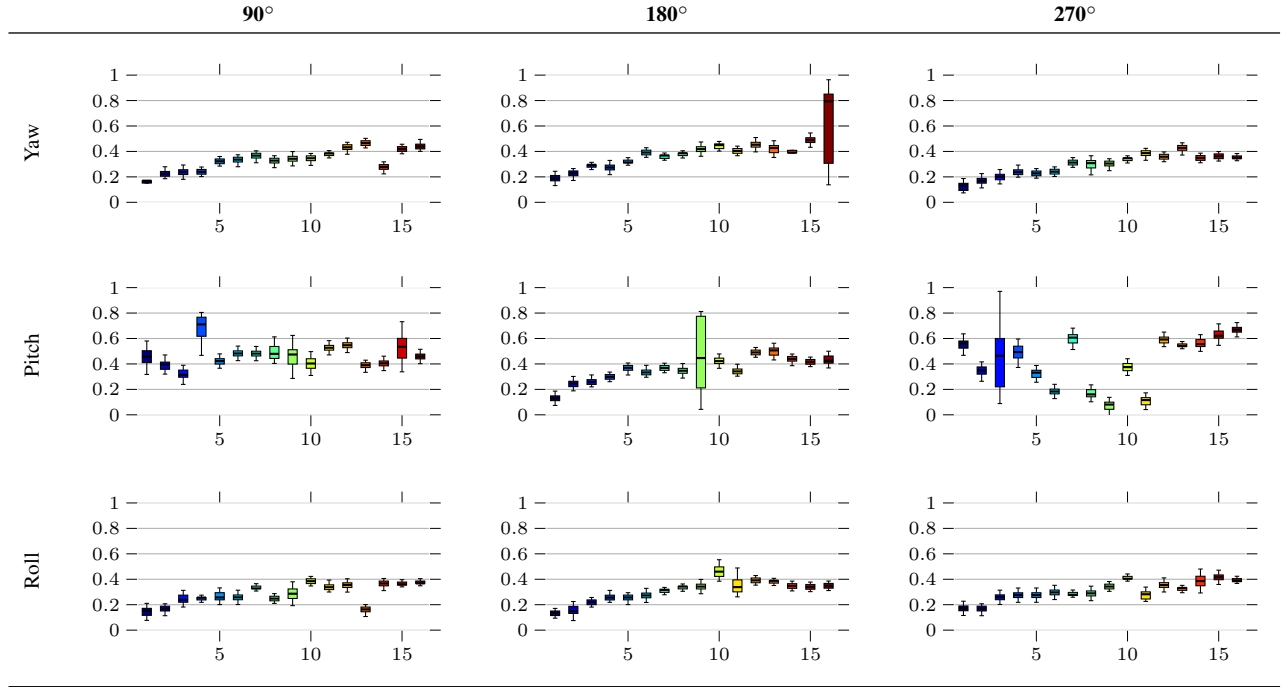


Fig. 7: UWB node localization for two moving UWB Initiators implementing a Least Square Estimator outside the convex envelope alongside the absolute position error.

using the measured distances. The results for two scenarios can be seen in Figure 6 and Figure 7. In both cases the search windows and step size parameters are the same, showing different results for each. Figure 6a shows a closer match of the calculated position to the ground truth than in Figure 7a. Both Figure 6b and Figure 7b clearly show the same, with the first case showing a lower error than the second. This demonstrates the influence of being inside or outside the convex envelope and is the reason for including both types of scenarios in our dataset.

C. Algorithm comparison

Case III presents scenarios with eight static UWB nodes, that provide the distances all-to-all as seen in Figure 4. For each scenario we implemented two relative localization

algorithms used in our previous research [22]. The first algorithm is multilateration (MLAT), which uses all the measured distances, and the second is Gradient Descent optimization (GD) to minimize distance error. Both localization approaches are further detailed in [22]. Figure 8 shows the results for both MLAT and GD for three scenarios. It also shows the error of each UWB node position according to the algorithm.

The three configurations were selected because they present challenges for localization solutions, such as aligning nodes or forming 90° angles. Figure 8a shows how both algorithms present different results. GD performs noticeably better than MLAT. It can be more appreciated in Figure 8b, where most of the higher errors for each node are from MLAT. Figure 8c present more mixed results, with Figure 8d showing that some nodes perform better with MLAT than GD and vice versa. Finally, Figure 8e and Figure 8f show MLAT with better results than GD.

With these three UWB node formations, we can observe that different algorithms perform better or worse depending on the scenario. For this reason, we included different formations in the dataset, to analyze the advantages and disadvantages of various localization methods. Furthermore, it helps to study algorithms' performance in edge case scenarios like with all UWB nodes in a straight line.

VI. CONCLUSION

We have presented a novel dataset for UWB for both characterization and UWB-based localization. For characterization, we focused on error analysis for different distances at different rotations. We showed how the distances and the angle of rotations affect the UWB errors obtained. Regarding localization, we presented four different cases, two from previous

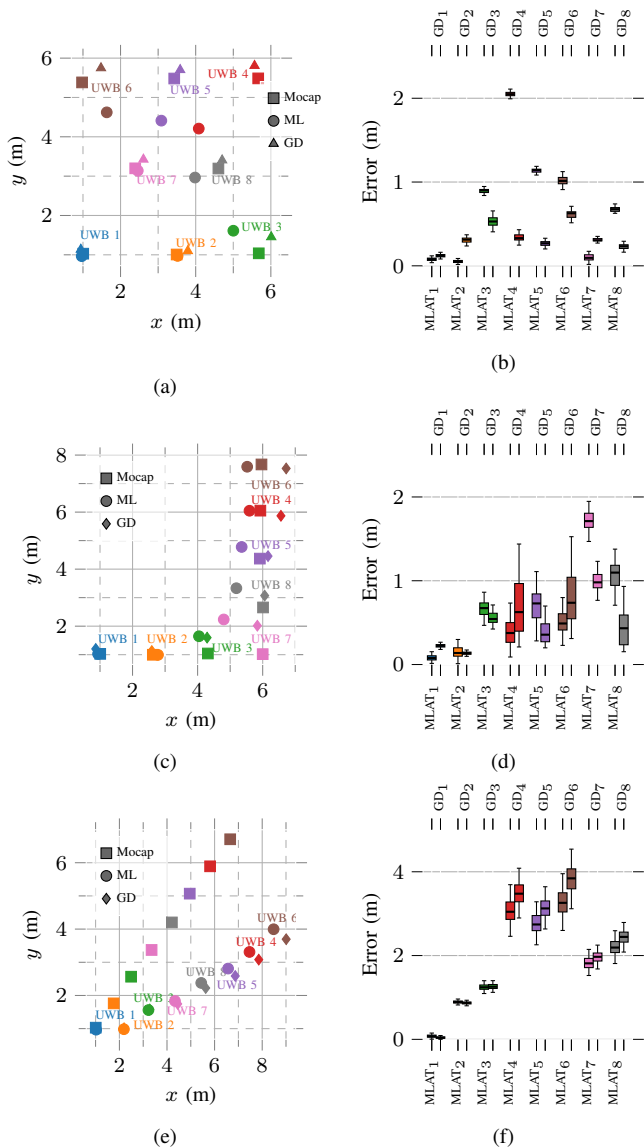


Fig. 8: Localization results for the implementation of a multilateration algorithm and a Gradient Descent Optimization algorithm for the three configurations presented in the dataset, alongside their absolute distance errors.

works, and two analyzed in this work. We included scenarios in our dataset to study the influence of the convex envelope for relative localization with responders in different locations. We also provide different UWB formations for the study of relative localization algorithms, especially in challenging configurations. We presented two solutions and analyzed their

We believe that the dataset presented in this paper can enable the research community to further explore the limitations of relative localization solutions using UWB. When confronted with multiple node configurations and challenging positions. Future work will focus on implementing a robust localization solution for infrastructure-free relative localization by studying different localization solutions in real-time.

results.

ACKNOWLEDGMENT

This research work is supported by the Academy of Finland's AeroPolis project (Grant No. 348480) and by the R3Swarms project funded by the Secure Systems Research Center (SSRC), Technology Innovation Institute (TII).

REFERENCES

- [1] Hayat *et al.* Survey on unmanned aerial vehicle networks for civil applications: A communications viewpoint. *IEEE Communications Surveys & Tutorials*, 18(4), 2016.
- [2] B. Alsalam *et al.* Autonomous uav with vision based on-board decision making for remote sensing and precision agriculture. In *2017 IEEE Aerospace Conference*. IEEE, 2017.
- [3] Plaksina *et al.* Development of a transport robot for automated warehouses. In *2018 International Multi-Conference on Industrial Engineering and Modern Technologies (FarEastCon)*. IEEE, 2018.
- [4] Albeaino *et al.* Trends, benefits, and barriers of unmanned aerial systems in the construction industry: a survey study in the united states. *J. Inf. Technol. Constr.*, 26, 2021.
- [5] Y. Lu *et al.* A survey on vision-based uav navigation. *Geo-spatial information science*, 21(1), 2018.
- [6] T. Qin *et al.* Vins-mono: A robust and versatile monocular visual-inertial state estimator. *IEEE Transactions on Robotics*, 34(4), 2018.
- [7] T. Qin *et al.* A general optimization-based framework for local odometry estimation with multiple sensors, 2019.
- [8] Qi *et al.* Cooperative 3-d relative localization for uav swarm by fusing uwb with imu and gps. In *Journal of Physics: Conference Series*, volume 1642. IOP Publishing, 2020.
- [9] Paneque *et al.* Multi-sensor 6-dof localization for aerial robots in complex gnss-denied environments. In *IEEE/RSJ IROS*. IEEE, 2019.
- [10] Peña Queralta *et al.* Uwb-based system for uav localization in gnss-denied environments: Characterization and dataset. In *IEEE/RSJ IROS*. IEEE, 2020.
- [11] Torrico Morón *et al.* Towards large-scale relative localization in multi-robot systems with dynamic uwb role allocation. In *ICRAE*, 2022.
- [12] Faheem Zafari, Athanasios Gkeliias, and Kin K Leung. A survey of indoor localization systems and technologies. *IEEE Communications Surveys & Tutorials*, 21(3), 2019.
- [13] Siyuan Chen, Dong Yin, and Yifeng Niu. A survey of robot swarms' relative localization method. *Sensors*, 22(12), 2022.
- [14] Bregar *et al.* Improving indoor localization using convolutional neural networks on computationally restricted devices. *IEEE Access*, 6, 2018.
- [15] Li *et al.* Accurate 3d localization for mav swarms by uwb and imu fusion. In *ICCA*. IEEE, 2018.
- [16] Barral *et al.* Multi-sensor accurate forklift location and tracking simulation in industrial indoor environments. *Electronics*, 8(10), 2019.
- [17] U. Raza *et al.* Dataset: Indoor localization with narrow-band, ultra-wideband, and motion capture systems. In *Proceedings of the 2nd Workshop on Data Acquisition To Analysis*, 2019.
- [18] Delamare *et al.* A new dataset of people flow in an industrial site with uwb and motion capture systems. *Sensors*, 20(16), 2020.
- [19] Vey *et al.* Indoor uwb localisation: Locura4iot testbed and dataset presentation. In *LCN*. IEEE, 2022.
- [20] Gao *et al.* A particle swarm optimization based multilateration algorithm for uwb sensor network. In *2009 Canadian Conference on Electrical and Computer Engineering*. IEEE, 2009.
- [21] Ridolfi *et al.* Uwb anchor nodes self-calibration in nlos conditions: A machine learning and adaptive phy error correction approach. *Wireless Networks*, 27(4), 2021.
- [22] Salimpour *et al.* Exploiting redundancy for uwb anomaly detection in infrastructure-free multi-robot relative localization. *arXiv preprint arXiv:2303.17207*, 2023.
- [23] Yu *et al.* Loosely coupled odometry, uwb ranging, and cooperative spatial detection for relative monte-carlo multi-robot localization. *arXiv preprint arXiv:2304.06264*, 2023.